The 11th Canadian Conference on Earthquake Engineering
Canadian Association for Earthquake Engineering

STRUCTURAL PERFORMANCE OF BEAM-COLUMN JOINT USING DFRCC

Naoya SANO
Master Program, Dept. of Engineering Mechanics and Energy, University of Tsukuba, Japan
s1420894@u.tsukuba.ac.jp

Hiroshi YAMADA
Master Program, Dept. of Engineering Mechanics and Energy, University of Tsukuba, Japan
s1520931@u.tsukuba.ac.jp

Masaru MIYAGUCHI
Master Program, Dept. of Engineering Mechanics and Energy, University of Tsukuba, Japan
s1420932@u.tsukuba.ac.jp

Akira YASOJIMA, Ph.D.
Assistant Professor, Dept. of Engineering Mechanics and Energy, University of Tsukuba, Japan
yasojima@kz.tsukuba.ac.jp

Toshiyuki KANAKUBO, Ph.D.
Associate Professor, Dept. of Engineering Mechanics and Energy, University of Tsukuba, Japan
kanakubo@kz.tsukuba.ac.jp

ABSTRACT: In this study, the loading test of precast beam-column joints using DFRCC in panel zone was conducted to evaluate the effect of the shear performance of joint panel with DFRCC. The experiment factor is the fiber (PVA) volume fraction in mortal matrix at panel zone. From the experiment result, it can be recognized that the fiber could inhibited the damage of panel zone. According to the image analysis of observed cracks at panel zone, shear force which is carried by fibers can be calculated from the bridging law of PVA fiber. The calculated shear force shows an agreement with the increment of shear force of the specimen with fiber. This result indicates that the shear force carried by fibers can be evaluated by the behavior of cracks at panel zone.

1. Introduction

Rationalization of workmanship is demanded on precast (PCa) concrete buildings. Up to now, while PCa members have been utilized for beams or columns, beam-column joints in PCa systems have been cast in situ. Recently, developments and researches for new PCa systems, in which the panel zone of the beam-column joint is manufactured as the PCa members together with the PCa beams (Fig. 1), have been carried out. The previous paper reported that the structural performance of beam-column joints produced by the proposed PCa system showed the similar one with the conventional beam-column joints cast-in-situ (Hosoya et al., 2012). However, when the safety margin of shear capacity of joint panel is close to 1.0, shear failure occurs at panel zone after the flexural yielding of beams. Ductility becomes worse due to the slip behavior subjected to a large deformation.

On the other hand, many researches on ductile fiber-reinforced cementitious composites (DFRCC), which can improve the ductility of concrete, have been carried out in recent years (Japan concrete institute,

2012). Previous study reported that the shear capacity of the beams using DFRCC is higher than that of ordinary concrete beams (Shimizu et al., 2004). The authors also studied that using DFRCC in panel zone can improve ductility of beam-column joints after flexural yielding (Sano et al., 2014). In order to complete the structural design of beam-column joint using DFRCC, however, the further research on evaluating the shear capacity of beam-column joints is necessary. In this study, the loading test for beam-column joints using DFRCC in panel zone, which are designed to fail by shear failure in panel zone before flexural yielding, is conducted to evaluate the shear capacity of joint.

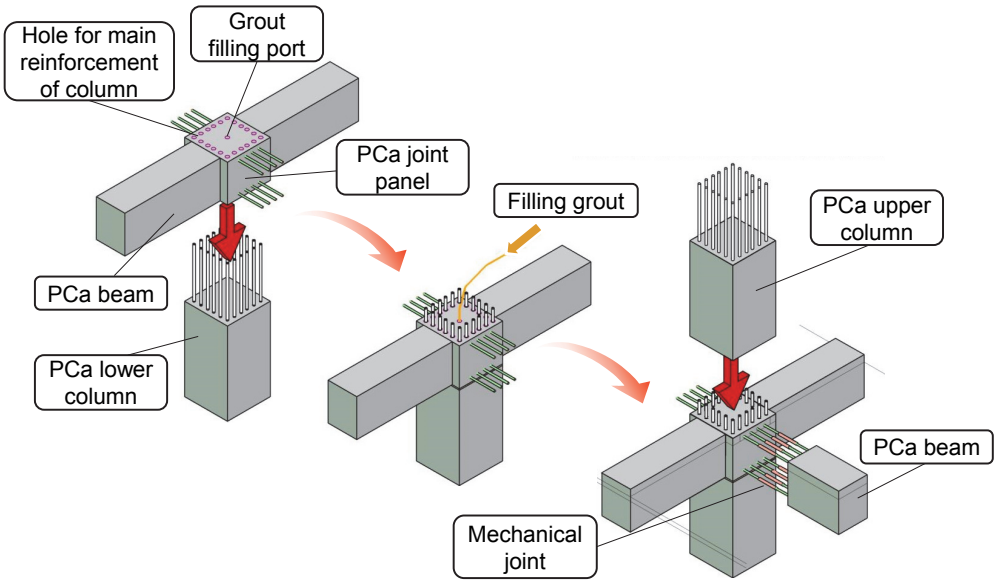

Fig. 1 – PCa system

2. Experimental Program

2.1. Test Specimens

Specimens are listed in Table 1. Fig. 2 shows the dimention of the specimens. The internal beam-column joint in high-rise RC buildings is scaled with the beam section of 380 mm x 420 mm and the column section of 500 mm x 500 mm. To evaluate the shear capacity of joint panel, the specimens are designed to fail by shear in panel zone before flexural yielding. The safety margin of shear capacity of joint panel is set at approximately 0.6 using high strength longitudinal bars (USD685). The experimental factor is the fiber volume fraction in DFRCC at panel zone. No.24 is without fiber, while No.25 within the fiber volume fraction which is set to 1.0 %. In order to obtain the effect on the shear capacity by only fibers in DFRCC, the hoops are not arranged in panel zone. Moreover, the bar-joints and sheaths, which are ordinary required in PCa system, are not arranged for easy making of specimens.

Mechanical properties of fibers used in DFRCC are summarized in Table 2. The results of material tests for concrete, DFRCC and reinforcing bars are summarized in Table 3 and Table 4. The compression test and splitting test were carried out with the cylinder test pieces (ϕ100 mm x 200 mm). In case of DFRCC, the splitting tensile strength is regarded as the peak load when the first crack initiates.

Table 1 – Specimen list

ID	Target strength (MPa)	Fiber volume fraction (%)	Beam		Column	
			Longitudinal reinforcing bar	Stirrup	Longitudinal Reinforcing Bar	Hoop
No.24	40	0.0	18-D22 (USD685)	6-D10@60 (SD785)	16-D22 (USD685)	6-D10@60 (SD785)
No.25		1.0				

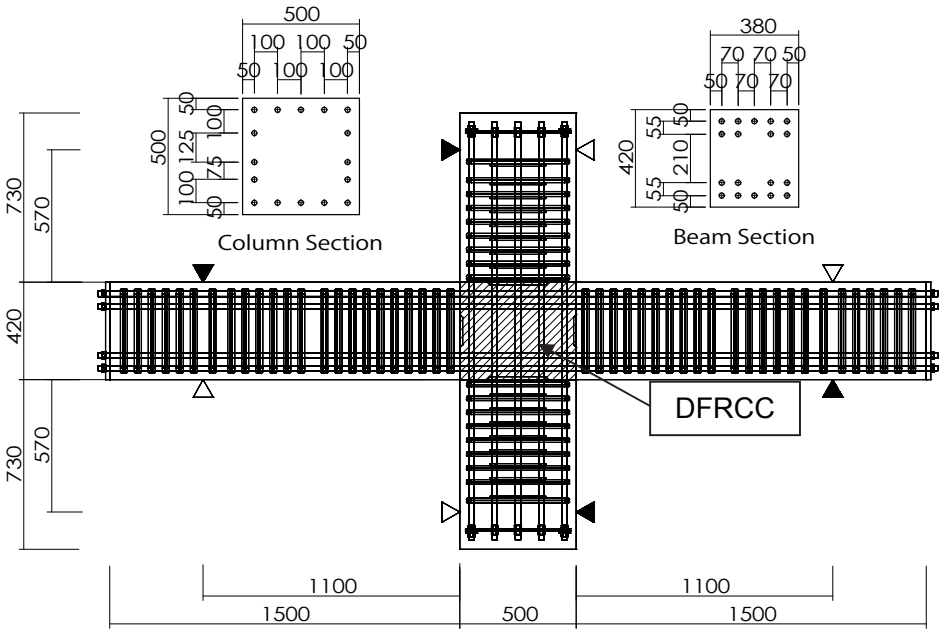

Fig. 2 – Specimen dimensions

Table 2 – Mechanical properties of fiber

Fiber	Length (mm)	Diameter (mm)	Tensile strength (MPa)	Elastic modulus (GPa)
PVA	12.0	0.10	1200	28

Table 3 – Mechanical properties of concrete and DFRCC

Type	Specimen No	Place	Compressive strength (MPa)	Splitting tensile strength (MPa)	Elastic modulus (GPa)
Concrete	No.24	Beam	39.9	3.55	29.6
	No.25	Column	39.1	3.42	28.0
DFRCC	No.24	Panel Zone	50.3	2.55	17.6
	No.25		52.5	2.57	17.1

Table 4 – Mechanical properties of bar

Type	Diameter	Specimen No	Place	Yield strength (MPa)	Tensile strength (MPa)	Elastic modulus (GPa)
USD685	D22 (22 mm)	No.24 No.25	Longitudinal reinforcing bar	717	900	195
SD785	D10 (10 mm)		Stirrup and hoop	832	996	218

2.2. Loading Method and Measurement

The column was supported by oil jacks and the story drift angle was controlled by the actuators attached to the inflection point of the beams. The reversed cyclic loading was applied with the target story drift angles of R = ±1/400, ±1/200, ±1/100, ±1/67, ±1/50, ±1/33, ±1/25, ±1/20 and +1/14 rad.

Fig. 3 and Fig. 4 show the setups of LVDT. The measuring items were the applied load to beams, story drift (Fig. 3), deformations of columns and beams, and local deformations around the panel zone (Fig. 4) and strains of the longitudinal bars. In addition, for specimen No.25, to observe shear cracks behavior in panel zone, photos were taken in every 10 second using two cameras during the loading (details are explained in Chapter 4).

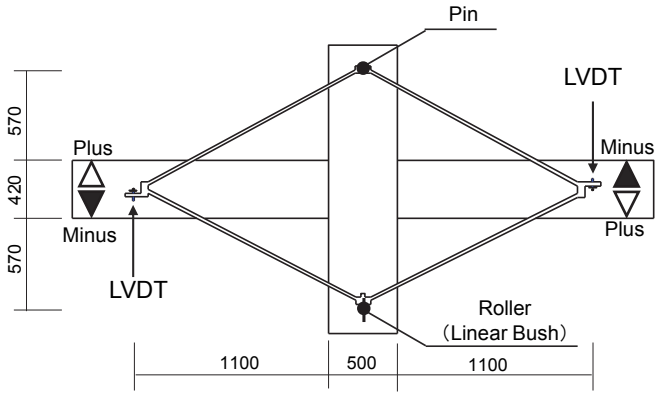

Fig. 3 – Measurement of story drift

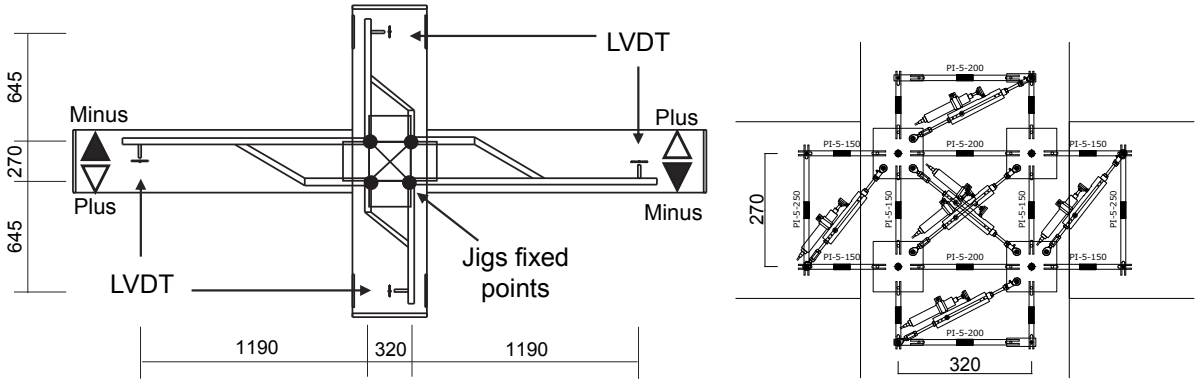

Fig. 4 – Measurement of local deformation

3. Experimental Result

3.1. Load-Story Drift Angle Curve and Failure Mode

Fig. 5 shows the relationship between the applied load to beam and the story drift angle, and Fig. 6 shows the crack patterns of the panel zone at the maximum load. Shear cracks in panel zone, bending cracks at the end of the beams and shear cracks in beams occurred in both two specimens. After that, the shear crack width in panel zone increased. The maximum load was observed at 1/50 rad. of story drift angle.

After the maximum load, the shear crack width in panel zone of specimen No.24 increased. And the peak load started decreasing due to shear failure in panel zone. On the other hand, although the shear cracks in panel zone of specimen No.25 became wider, the peak load started decreasing due to compression failure at the ends of the beams and columns. From the results, it can be observed that the damage of joint panel is inhibited by using DFRCC in panel zone.

The maximum load of specimen No.24, which is without fiber in panel zone, is 389 kN, and that of specimen No.25, in which the fiber is mixed in panel zone, is 459 kN. It is considered that the shear capacity of joint panel can be improved by the effect of fiber bridging.

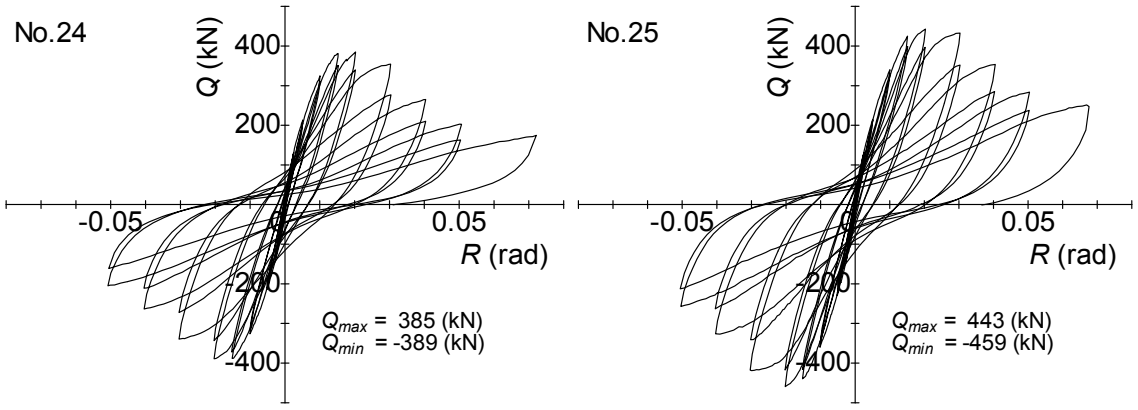

Fig. 5 – Load - story drift angle curve

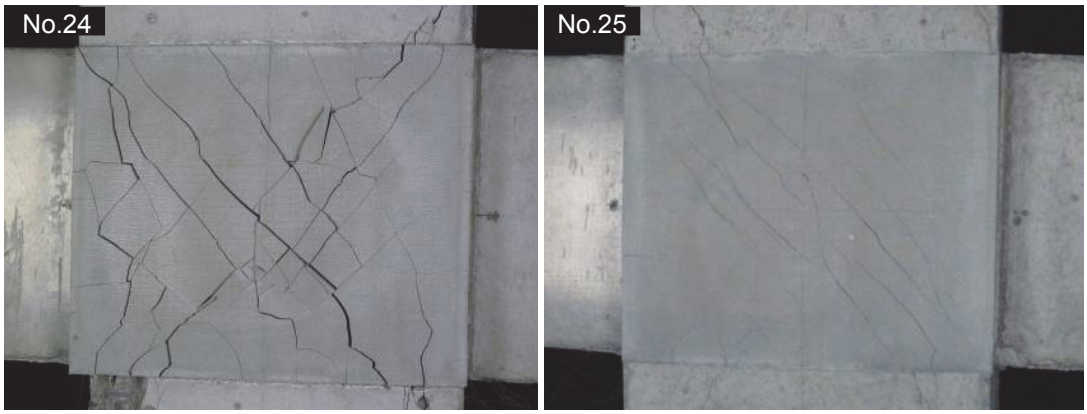

Fig. 6 – Crack pattern at maximum load

3.2. Local deformations

Fig. 7 shows the transition of deformations of panel zone, columns and beams. Each deformation is expressed by the conversions into ratio to the story drift. In both specimens, the similar tendency that the ratio of panel zone increases until story drift reaches 1/50 rad. After the maximum load, the ratio of panel zone of specimen No.24 increases while that of No.25 shows reduction and the ratio of column increases. The deformation of panel zone of specimen No.25 is smaller than that of No.24 because the fiber prevents the panel shear cracks increasing.

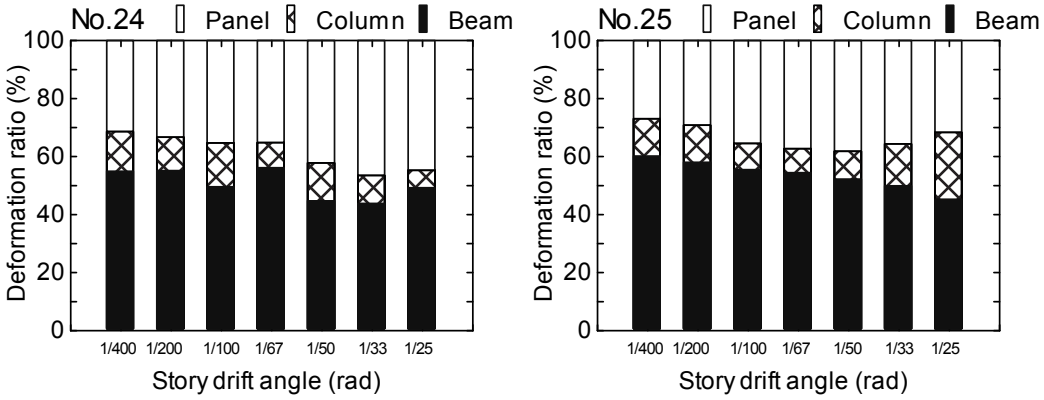

Fig. 7 – Deformations of panel, column and beam

4. Crack Behavior in Panel Zone

4.1. Method of Observation

To evaluate the shear cracks in panel zone of specimen No.25, the mesh with 10 mm x 10 mm intervals was drawn on the surface in panel zone and photos were taken by two cameras as shown in Fig. 8. The target regions for photos were center and corner area (120 mm x 80 mm) enclosed by the longitudinal bars of columns and beams in panel zone. Fig. 8 also indicates the observed cracks which are focused for calculating the shear force carried by fibers. The pixel number of used camera gives that 1 pixel corresponds to 0.02 mm square. The photos were taken in every 10 second considering the data measuring intervals and the loading speed (about 3 mm per minute).

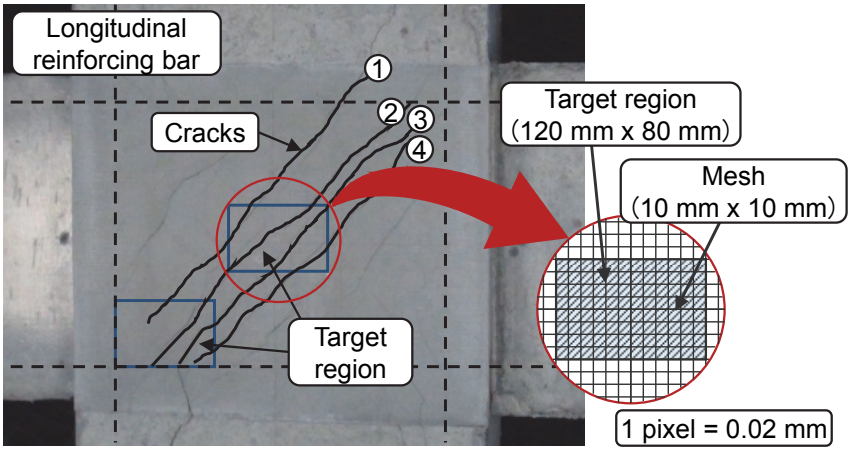

Fig. 8 – Observation of cracks

4.2. Crack Width and Principal Strain Angle

Fig. 9 shows the calculation methods of crack width. It is considered that the stress field in panel zone is in a biaxial stress field in which tensile stress and shear stress exist along shear crack. The crack width is defined as the relative displacement between two points printed in same mesh line. Crack opening and crack sliding is defined as the normal displacement and the perpendicular movement between two points, respectively. Principal strain is calculated by Mohr's strain circle.

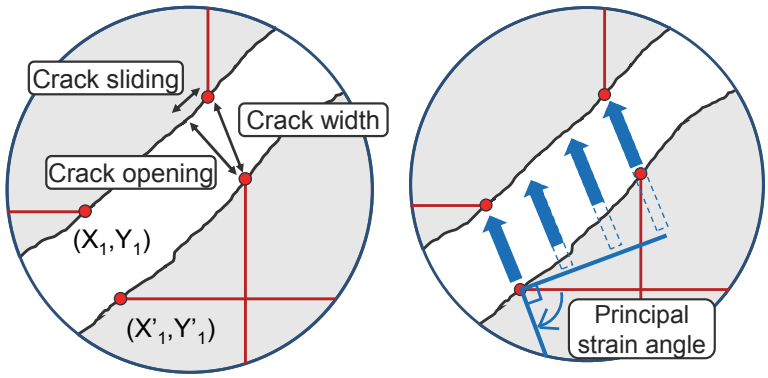

Fig. 9 – Calculation method of crack width and principal strain angle

Fig. 10 - Fig. 12 show the transition of crack width, crack opening and crack sliding of crack #4 shown in Fig. 8. The plotted marks are grouped into each loading cycle with target story drift angle shown in the figures. The crack width increases as the story drift also increases. The width reaches approximately 0.8 mm at maximum load in 1/50 rad. of story drift angle. The residual crack width, which is indicated near Y-axis, increases, as the target story drift angle rises, while increment rate shows gradual slope. After the maximum load, the crack width converges at around 0.9 mm. The crack opening and the crack sliding also increases as the story drift increasing similarly with crack width. At the maximum load, the crack opening and crack sliding is approximately 0.7 mm and 0.3 mm, respectively. It is considered that the increase of crack width in panel zone is mainly affected by tensile stress acting on crack surface. After the maximum load, the crack opening does not so increase and it converges at around 0.8 mm. On the other hand, the crack sliding increases after maximum load and reaches around 0.4 mm at 1/25 rad. of story drift angle. It is considered that the crack width increases due to shear stress after maximum load. The crack width, opening and sliding decrease in the second cycle of 1/25 rad. because of the increment of deformation of columns and beams.

Fig. 13 shows the relationship between the principal strain angle and the story drift angle. At the loading cycle of 1/100 rad. of target story drift angle, the principal strain angle varies around 60 degree. After the loading cycle of 1/67 rad., the scattering of the angle become smaller. It converges at a certain value in each cycle. The convergent angle decreases gradually as the cycle increases. The angle is around 30 degree and 20 degree at the loading cycle of 1/50 rad. and at second cycle of 1/50 rad., respectively. The angle does not show remarkable change after those cycle.

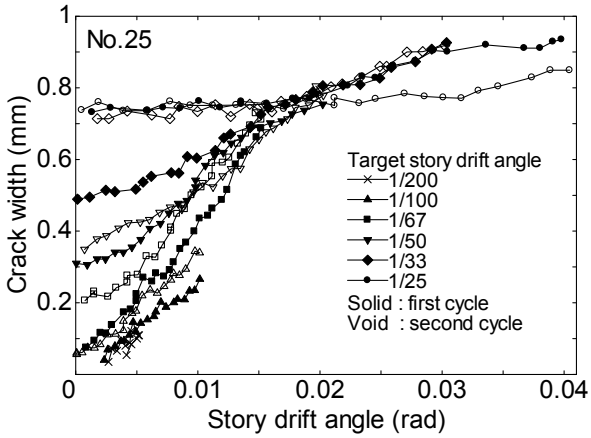

Fig. 10 – Crack width - story drift angle relationship

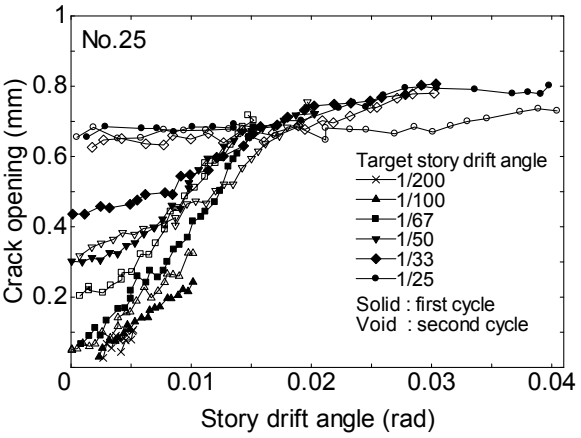

Fig. 11 – Crack opening - story drift angle relationship

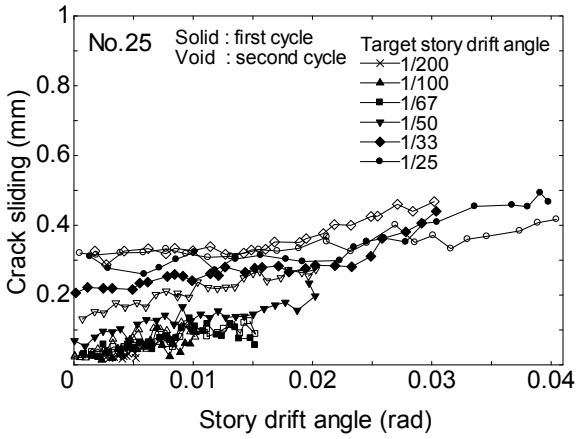

Fig. 12 – Crack sliding - story drift angle relationship

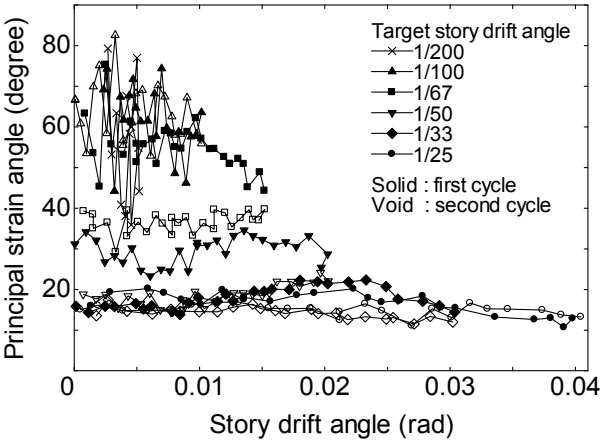

Fig. 13 – Principal strain angle - story drift angle relationship

5. Shear Force Carried by Fiber

5.1. Calculation Method

The calculation method of shear force by fiber is presented in Fig. 14. The shear force by fiber bridging is determined by the crack width and the principal strain angle explained before. The tensile stress and tensile force are calculated by these values, which are obtained as the average of next points in one crack. The sectional area acting these stresses is defined as area between the two points.

The bridging law (the upper right figure in Fig. 14) is adopted for calculating the tensile stress carried by fiber at cracks in DFRCC (Asano and Kanakubo, 2014). The bridging stress is calculated based on the assumption that the fiber randomly orients.

The tensile force is estimated from tensile stress using the principal strain angle. The sectional area acting tensile stress is assumed using crack length between mesh lines and the principal strain angle. Tensile stress multiplied by sectional area gives tensile force.

The shear force carried by fiber is the component of tensile force. All forces in each mesh are summed. The extrapolated values are assumed in the out of the photo area.

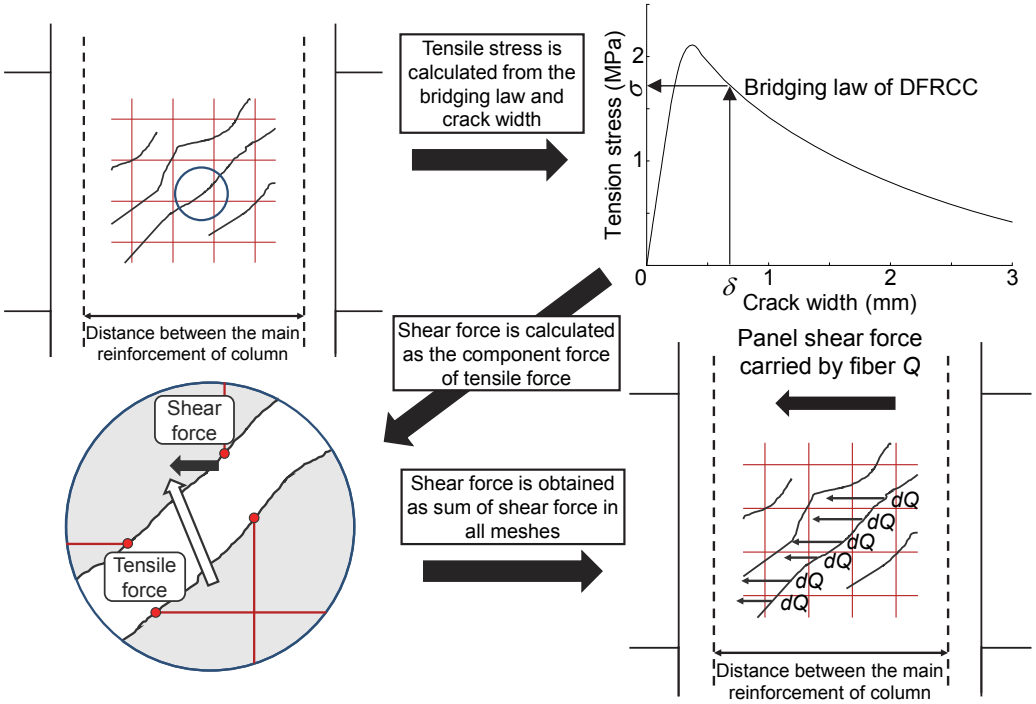

Fig. 14 – Deriving Process of Fiber Shear Force

5.2. Predicted Shear Force

Fig. 15 and Fig. 16 show the relationship between the calculated shear force and the story drift angle. The calculation results for each crack shown in Fig. 8 are shown in Fig. 15, and the average value of those is shown in Fig. 16. The shear force difference between specimen No.25 and No.24 is also shown in the graph.

The transition of the shear force carried by fiber for each crack shows similar tendency upto 1/100 rad. After that, the shear force carried by fiber at crack #3 and #4 becomes larger due to deformation localization. It is considered that there is the increment and decrement of shear force crack by crack. The average of the shear force carried by fiber shows similarity with the shear force difference between No.24 and No.25 upto 1/50 rad. After 1/50 rad., difference between No.24 and No.25 becomes larger than calculated value because of compression failure at the ends of beams and columns.

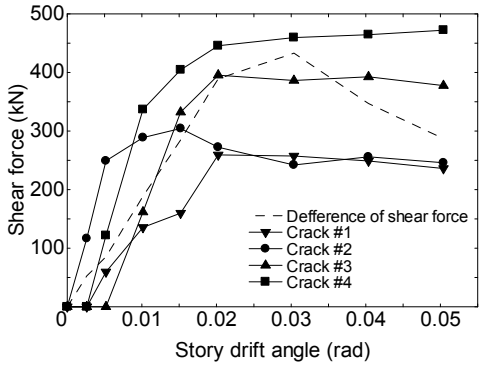

Fig. 15 – Shear force carried by fiber

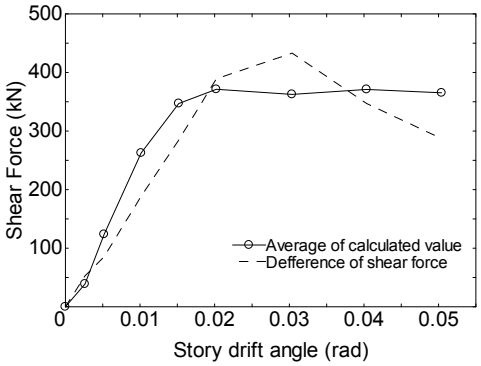

Fig. 16 – Averaged shear force carried by fiber

6. Conclusion

In this study, the shear behavior of beam-column joint was examined by loading test for the specimen using DFRCC in panel zone. The damage of joint panel was inhibited by DFRCC and the maximum load increased by the effect of fiber bridging. The shear force carried by fiber was estimated based on bridging law of DFRCC and the observed crack width and the principal strain angle of shear cracks. It shows a similar tendency with the shear force increment obtained by DFRCC specimen. It is considered that the shear force by fiber can be calculated by evaluating the behavior of cracks at panel zone.

7. Acknowledgement

The authors wish to express their gratitude and sincere appreciation to the Kuraray Co., Ltd. for providing the PVA fiber. This study was supported by the JSPS KAKENHI Grant Number 26289188.

8. References

ASANO Kohei and KANAKUBO Toshiyuki, “Study on Fiber Bridging Constitutive Law in Consideration of Fiber Orientation in High Performance Fiber Reinforced Cementitious Composites”, *Summaries of technical papers of annual meeting Architectural Institute of Japan,* Materials and Construction, 2014, pp. 185-186. (in Japanese)

HOSOYA Hiroshi, MATSUMOTO Masashi, KANAKUBO Toshiyuki and YASOJIMA Akira, “Experimental Study on Structural Performance of Precast RC Beam-Column Joints”, *AIJ Journal of Technology and Design*, Vol. 18, No. 39, 2012, pp. 529-534. (in Japanese)

JAPAN CONCRETE INSTITUTE, “Technical Committee Report on Innovation Application of Fiber Reinforced Cementitious Composites”, *Committee Report JCI-TC-104A,* 2012. (in Japanese)

SANO Naoya, KIMURA Taichi, KANAKUBO Toshiyuki, YASOJIMA Akira and HOSOYA hiroshi, “Structural Performance of Precast Concrete Beam-Column Joints Using DFRCC in Joint Panel”, *Summaries of technical papers of annual meeting Architectural Institute of Japan,* Structures IV, 2014, pp. 419-420. (in Japanese)

SHIMIZU Katsuyuki, KANAKUBO Toshiyuki, KANDA Tetsushi and NAGAI Satoru, “Shear Behavior of Steel Reinforced PVA-ECC Beams”, *13th World Conference on Earthquake Engineering,* Conference Proceedings DVD, Paper No. 704, 2004.